Science and Technology of Advanced Materials

ISSN: (Print) (Online) Journal homepage: www.tandfonline.com/journals/tsta20

Naphthalimide-based fluorescent polymeric probe: a dual-phase sensor for formaldehyde detection

Subhadip Roy, Swagata Pan, Swaminathan Sivaram & Priyadarsi De

To cite this article: Subhadip Roy, Swagata Pan, Swaminathan Sivaram & Priyadarsi De (21 Feb 2025): Naphthalimide-based fluorescent polymeric probe: a dual-phase sensor for formaldehyde detection, Science and Technology of Advanced Materials, DOI: 10.1080/14686996.2025.2469493

To link to this article: https://doi.org/10.1080/14686996.2025.2469493

Publisher: Taylor & Francis & The Author(s). Published by National Institute for Materials Science in partnership with Taylor & Francis Group.
Journal: *Science and Technology of Advanced Materials*
DOI: 10.1080/14686996.2025.2469493

Naphthalimide-based Fluorescent Polymeric Probe: A Dual-Phase Sensor for Formaldehyde Detection

Subhadip Roy,[1] Swagata Pan,[1] Swaminathan Sivaram[2,*] and Priyadarsi De[1,*]

[1]Polymer Research Centre and Centre for Advanced Functional Materials, Department of Chemical Sciences, Indian Institute of Science Education and Research Kolkata, Mohanpur-741246, Nadia, West Bengal, India.

[2]Indian Institute of Science Education and Research Pune, Dr. Homi Bhabha Road, Pune - 411008, India.

*Corresponding authors: emails: s.sivaram@iiserpune.ac.in (SS); p_de@iiserkol.ac.in (PD)

ABSTRACT

Formaldehyde (FA) is a common pollutant found indoors and outdoors, posing a significant threat to human health. Therefore, developing sensitive and efficient detection methods for FA is essential for environmental monitoring and protecting public health. Herein, we report a naphthalimide-conjugated water-soluble polymeric fluorescent probe for the detection of FA in both aqueous and vapor phases using fluorimetric methods. The aromatic amines present in the side chain of the polymer react with FA, forming a Schiff base (imine bond). This imine formation inhibits the photoinduced electron transfer (PET) process within the polymer, leading to a "turn-on" fluorescence under 365 nm UV light. The probe is capable of selectively sensing FA with a detection limit as low as 1.36 nM in aqueous medium. The formation of imine is confirmed for the model reaction between 6-(4-aminophenyl)-2-(4-((4-vinylbenzyl)oxy)phenyl)-1H-benzo[de]isoquinoline-1,3(2H)-dione and FA by electrospray ionization mass spectrometry (ESI-MS) and nuclear magnetic resonance (NMR) titration methods. The mechanism behind "turn-on" FA sensing is investigated using density functional theory (DFT) analysis. Additionally, the study demonstrates a facile approach for covalently attaching the polymer on the surface of a filter paper surface *via* ultraviolet (UV) light-induced cross-linking. Such polymer attached paper exhibits FA vapor sensing through changes in fluorescence intensity.

KEYWORDS: Formaldehyde, polymeric probe, fluorometric sensing, schiff-base formation, aqueous and vapor phase detection

Article classification: Sensors and actuators

1. Introduction

Formaldehyde (FA), one of the most reactive carbonyl species, is widely utilized as a basic raw material in building construction, paints and coatings, furniture making, textile production, and the chemical industry [1]. Formaldehyde production exceeds 20 million tons per annum and has emerged as a major environmental risk since its inhalation can lead to serious health-related concerns [2]. Moreover, FA inhalation promotes the growth of squamous cell carcinomas in rats' nasal passages and nasopharyngeal cancer in humans [3]. The International Agency for Research on Cancer (IARC) has classified FA as a Group 1 carcinogen for both humans and animals [4]. Typically, 750 ppb is the standard permissible exposure limit set by the Occupational Safety and Health Administration (OSHA), while 20 ppm is considered the highest exposure value, which is immediately dangerous to life or health (IDLH) [5]. Beyond its well-known man-made origins, FA is also produced inside organisms, where it plays a variety of physiological and pathological activities [6]. FA content in biological systems can be influenced by both exogenously delivered and endogenously generated sources. Consequently, elevated cellular FA levels have been associated with a range of chronic disorders, including heart disease, leukemia [7], diabetes [8], Alzheimer's disease [9], and numerous malignancies.

Recently, significant efforts have been devoted towards the development of formaldehyde sensing methods, including potentiometry [10], mass spectrometry [11], electrochemical analysis [12], etc. Among these, fluorescence-based techniques have emerged as the most promising approach because of their ease of use and high detection sensitivity, drawing widespread interest from the scientific community. To date, numerous small molecule-based fluorescent sensors have been designed for formaldehyde sensing, based on FA amine condensation [13], hydrazine (-NH-NH_2) condensation [14,15], and aza-Cope rearrangement reaction [16]. However, these small molecular probes contain hydrophobic organic chromophores, resulting in poor water solubility and limiting their applications in aqueous medium and biological environments [17]. Consequently, performing sensing experiments needs volatile and hazardous organic solvents or hybrid aqueous solutions, which significantly reduce their utility in applications [18,19]. Therefore, developing a water-soluble probe with a lower limit of detection (LOD) and rapid sensing capability is essential for precise and quantitative measurement of FA in both biological and environmental milieu.

In this regard, water-soluble fluorescent polymeric probes have emerged as a promising alternative, providing a broad range of potential advantages that overcome the challenges

associated with formaldehyde detection [20]. For example, Liu *et al.* designed a polymeric probe *via* the Hantzsch reaction, which detects endogenous FA in living cells [21]. Li and coworkers reported chitosan-based water-soluble polymers for FA detection in various food samples [22]. Also, a porous polymer composite was reported to remove gaseous FA *via* oxime bond formation at room temperature [23]. Recently, our group reported a side-chain tryptophan-based water-soluble polymeric probe to detect FA through a Pictet-Spengler cyclization reaction in an aqueous medium [24]. Although these polymeric probes detected FA in an aqueous medium, their applications to sensing FA in the vapor phase were not explored, possibly because of their long equilibrium time to detect FA quantitatively. Detection of gaseous FA and toxic volatile organic compounds (VOCs) is a crucial frontier in scientific and technological progress [25,26], essential for improving safety, environmental friendliness, and ease of handling [27]. Therefore, the design of sensitive and reliable polymeric sensors for FA vapor has gained much interest due to the demand for real-time monitoring of air quality and workplace safety [28,29]. To address these issues, we aimed to develop a water-soluble fluorescent polymeric probe to detect FA both in the aqueous and vapor phases through fluorogenic response.

To this end, naphthalimide-based water-soluble polymeric probe with amino groups in pendant naphthalimide moieties was synthesized using reversible addition-fragmentation chain transfer (RAFT) polymerization for rapid FA detection in both aqueous and vapor phases. Initially, naphthalimide was introduced as a signal reporting unit and functionalized with an amine group to facilitate binding with formaldehyde. The probe's design is based on a specific chemical reaction between FA and the aromatic amino group of the polymer, which results in a "turn-on" fluorescence response from the side-chain naphthalimide fluorophores. Therefore, the designed polymeric probe can take advantage of the synergistic effects of many recognition sites in the side chain *via* weak supramolecular interactions to efficiently "concentrate" low amounts of FA pollutants around the polymer's random coil chains [30]. With this innovative strategy, the addition-elimination reaction between FA and aromatic amino groups of naphthalimide-conjugated polymer is accelerated significantly, leading to a fluorescence enhancement within a minute and increased sensitivity. Furthermore, to make a paper strip-based sensor for FA vapor, benzophenone moiety was incorporated in the side chain of the polymer and cross-linked on filter paper *via* irradiation with ultraviolet (UV) light [31].

2. Results and discussion

To develop the polymeric FA-sensor, a naphthalimide-conjugated styrenic monomer (Scheme S1) was synthesized by multistep organic synthesis. Initially, 6-bromo-2-(4-((4-vinylbenzyl)oxy)phenyl)-1H-benzo[de]isoquinoline-1,3(2H)-dione (**C2**) was synthesized [32], and subsequently reacted with 4-amino boronic acid *via* Suzuki-Miyaura coupling reaction to develop aromatic amine-conjugated 6-(4-aminophenyl)-2-(4-((4-vinylbenzyl)oxy)phenyl)-1H-benzo[de]isoquinoline-1,3(2H)-dione (**C3**). Finally, the desired styrenic monomer, *tert*-butyl (4-(1,3-dioxo-2-(4-((4-vinylbenzyl)oxy)phenyl)-2,3-dihydro-1H-benzo[de]isoquinolin-6-yl)phenyl)carbamate (NDIST), was prepared by protecting the free aromatic amine group of **C3**. **C1**, **C2**, and **C3** were characterized using ^{1}H NMR spectroscopy and electrospray ionization mass spectrometry (ESI-MS) (Figure S1-S4). The final monomer **NDIST** was characterized using ^{1}H NMR, ESI-MS, attenuated total reflection Fourier transform infrared spectroscopy (ATR-FTIR), and ^{13}C NMR spectroscopy (Figure S5-S8).

[Insert Scheme 1]

To prepare a water-soluble FA-sensing polymeric probe with controlled molecular weight and narrow dispersity (*Đ*), RAFT copolymerization was employed using water-soluble 2-(dimethylamino)ethyl methacrylate (DMAEMA) and hydrophobic NDIST monomers, in the presence of 4-cyano-(dodecylsulfanylthiocarbonyl)sulfanylpentanoic acid (CDP) as a RAFT agent and 2,2′-azobis(isobutyronitrile) (AIBN) as a radical source, in *N*,*N*-dimethylformamide (DMF) at 70 °C (Scheme 1A). Two copolymers, **BCP5** and **BCP10** were synthesized by varying the molar ratio of DMAEMA and NDIST, keeping the molar ratio of [CDP]:[AIBN] constant at 1:0.2 (Table S1). The non-appearance of vinyl proton peaks between 5.2-6.7 ppm in the ^{1}H NMR spectrum (Figure 1A, bottom) confirmed the successful removal of monomers in the final copolymers. The composition of DMAEMA and NDIST in the copolymers was calculated by comparing the peak intensity of the benzylic protons of NDIST moiety at 5.15-5.20 ppm and the dimethyl protons (-N(CH_3)$_2$) peak from DMAEMA unit at 2.3 ppm (Table **S1**). The number average degrees of polymerization (*DP*) for both DMAEMA and NDIST in the copolymer was determined by comparing the integration values of chain end protons [-CH_2-(CH_2)$_9$-CH_3] of CDP at 0.8-0.9 ppm to the characteristic peaks of -N(CH_3)$_2$ protons at 2.3 ppm from DMAEMA units and benzylic protons from NDIST at 5.15-5.20 ppm, respectively. The calculated DP_{DMAEMA} and DP_{NDIST} of **BCP5** were 80 and 4, respectively. The number average molecular weight of the copolymers was

determined from ^{1}H NMR analysis ($M_{n,NMR}$) using the formula (Table **S1**): $M_{n,NMR}$ = [($DP_{DMAEMA} \times MW_{DMAEMA}$) + ($DP_{NDIST} \times MW_{NDIST}$) + molecular weight of CDP], where *MW* represents the molecular weight of the two monomers. The size exclusion chromatography (SEC) was performed to determine the *Đ* and number average molecular weight ($M_{n,SEC}$) of copolymers (Figure 1B and Table S1). The theoretical molecular weights ($M_{n,theo}$) of the copolymers were also determined and results are shown in Table **S1**. The $M_{n,theo}$, $M_{n,NMR}$ and $M_{n,SEC}$ values in Table **S1** match reasonably well with each other, indicating the controlled nature of RAFT copolymerization of DMAEMA and NDIST. Finally, to prepare the desired naphthalimide-functionalized polymeric probe with pendant aromatic amine groups, *tert*-butyloxycarbonyl (Boc) groups of both **BCP5** and **BCP10** were deprotected using trifluoroacetic acid (TFA) in dichloromethane (DCM) at room temperature. The resulting deprotected copolymers were labelled as **DCP5** and **DCP10**, respectively. The successful cleavage of Boc groups was verified by the disappearance of the characteristic protons peak of Boc group at ~1.4 ppm range in the ^{1}H NMR spectrum of **DCP5** (Figure 1A, top). Furthermore, both the **DCP5** and **DCP10** copolymers were nicely soluble in water.

With water-soluble aromatic amine-conjugated naphthalimide-based polymers in hand, we sought to investigate their performance towards FA sensing in an aqueous medium. Initially, the UV-Vis and fluorescence analyses were carried out on both polymers in water. **DCP5** exhibited two absorption maxima at 280 nm and 420 nm in an aqueous medium, referrers to the π-π^* and n-π^* transitions for the naphthalimide unit (Figure **1C**). Although both polymers were water-soluble, **DCP10** exhibited self-assembly in an aqueous medium due to the higher content of hydrophobic NDIST units (data not shown here), which could potentially increase the response time. Our primary focus is on rapid FA detection in aqueous media, so the self-assembly characteristics of **DCP10** were not extensively studied. Therefore, **DCP5** was chosen for further studies to prevent such complications. As shown in Figure 2A, the addition of 100 nM FA to the aqueous solution of **DCP5** resulted in a slight blue shift (8 nm) in the UV-Vis spectrum. A subtle color change from colorless to light yellow was also observed under normal light. However, **DCP5** exhibited a significant fluorogenic response upon FA treatment, where the polymer displayed an emission maximum at 580 nm when excited at 420 nm (Figure 2B).

[Insert Figure 1]

The presence of an aromatic amine group in the naphthalimide unit quenched the strong fluorescence of naphthalimide moiety *via* the photoinduced electron transfer (PET) process

[33]. However, upon the addition of an increasing amount of FA (10 to 100 nM), the fluorescent intensity at 580 nm gradually increased and reached the maximum in the presence of 100 nM FA (Figure 3A). The noticeable increment in fluorescence intensity indicated the significant halt of the PET process during the fast Schiff base reaction between FA and the **DCP5**. This shows that the polymeric probe can sense a very low concentration of FA with outstanding fluorescence enhancement. Although the FA sensing mechanism of the amine-functionalized **DCP5** is based on imine formation reaction processes, it is imperative to study the kinetic profiles after FA addition. Hence, the time-dependent fluorescence behavior of the polymeric probe towards FA was examined. The fluorescence experiments were performed within cuvettes in a meticulously controlled manner. Fluorescence spectra of the aqueous solution of the polymeric probe were recorded at different time intervals upon the addition of 100 nM FA. As demonstrated in Figure 3B, the polymeric probe showed a quick response within just 1 min, with the fluorescence emission intensity at 580 nm gradually increased and saturated within 10 min. The limit of detection (LOD) for the **DCP5** towards FA was determined as 1.36 nM (Figure S9) [34]. Additionally, the absolute quantum yield of **DCP5** increased from 1.15 % to 3.15% after reaction with FA (Figure S10). Enhancement in the fluorescence intensity does not directly translate to a proportional increase in quantum yield, as other factors are also involved (Inner-filter effects, excited-state interactions, fluorescence lifetime, etc.). In the fluorescence titration experiment with the model compound (**C3**), the addition of an increasing amount of FA (10 to 100 nM) gradually increased the fluorescent intensity at 580 nm (Figure S11).

[Insert Figure 2]

To explore the ideal sensing condition, the fluorescence response of **DCP5** (10 mM with respect to the functional naphthalimide unit) to FA was studied across a pH range from 2 to 9 (Figure 3C). Upon the addition of FA to **DCP5**, an enhancement in fluorescence intensity was observed between pH 2.0 to 7.4, with a remarkable increase in the range of pH 4.5 -7.4. These results imply that the reaction between the FA and the aromatic amine groups present in the side chain of the polymer is more efficient under neutral conditions, making it well-suited for standard applications under different conditions [35]. Furthermore, the sensing selectivity (Figure 3D) and photostability (Figure S12) of the **DCP5** probe were studied in an aqueous medium. As depicted in Figure 3D, only a small increase in fluorescence was observed for several potentially interfering analytes, including various common aldehydes and other chemical species, such as 4-methoxy benzaldehyde, 4-nitrobenzaldehyde,

benzaldehyde, formic acid, glyoxal, acetone, glucose, benzophenone, and acetaldehyde. These investigations implied the excellent selectivity of the **DCP5** probe towards FA. Moreover, the emission intensities of **DCP5** were nearly constant under specific experimental conditions (irradiation at 420 nm for 30 min), suggesting its photostability under photoirradiation and exposure to atmospheric conditions (Figure S12**)**.

[Insert Figure 3]

To confirm the FA sensing mechanism of the polymeric probes, we performed ^{1}H NMR titration experiments and ESI-MS analysis. Given the challenges of low resolution in polymeric spectra, we utilized **C3** as a model compound to capture the ^{1}H NMR titration spectra. This approach provided valuable insights into the interaction between the polymer and FA, allowing us to elucidate the underlying mechanism of sensing. In Figure S13, the stepwise addition of FA leads to the gradual disappearance of the -NH_2 proton signal at ~5.5 ppm, accompanied by the emergence of a new peak at 9.5 ppm, corresponding to the imine (-N=C***H***$_2$) group. In addition, a peak at *m/z* = 509.1913 was found in the ESI-MS analysis of the reaction mixture of **C3** and FA (Figure S14). These results evidenced the formation of Schiff base (imine bond) during the reaction of FA with **DCP5** in an aqueous medium.

After confirming the sensitivity and selectivity of **DCP5** for FA, the probe's reversibility was studied in the presence of bisulfite (HSO_3^-) [36]. As shown in Figure 4A, after the formation of **DCP5**-FA adduct, it was reacted with $NaHSO_3$, and the emission intensity returned to its initial level within 3 min, closely aligning with the fluorescence intensity of **DCP5**. This suggested the reversibility of the formation of imine moieties from the aromatic amine groups of **DCP5** and FA. It is envisaged that the HSO_3^- traps the free FA and disrupts the imine adduct present in the polymer, leading to the formation of free amine-containing polymeric probe **DCP5**. The reversibility of **DCP5** was investigated up to five cycles (Figure 4B). Thus, in addition to selective and sensitive detection of FA, the **DCP5** copolymer can be effectively reused in the solution phase for multiple cycles.

[Insert Figure 4]

To gain a thorough understanding of the sensing mechanism, density functional theory (DFT) calculation was conducted to evaluate the highest occupied molecular orbital (HOMO) and the lowest unoccupied molecular orbital (LUMO) of the NDIST repeating unit before and after the addition of FA. The HOMO energy of the NDIST (-5.739 eV) was higher than the HOMO energy (-6.142 eV) of the corresponding imine derivative, indicating the

PET process was interrupted by the imine formation, leading to a “turn-on” fluorescence response (Figure 5) [37].

[Insert Figure 5]

To employ the designed polymeric material for practical applications, the vapor phase detection of FA was carried out. It is well-reported that the benzophenone undergoes cross-linking in the presence of UV light (365 nm) [31]. Thus, a terpolymer was prepared using benzophenone-based monomer (BPMA), NDIST, and DMAEMA, following RAFT polymerization (Scheme **S2**). To attain covalent attachment onto filter paper, the BPMA-containing terpolymer was dissolved in methanol (5 mg/mL). Subsequently, the paper was coated with the polymer solution by dip-coating (submerging for 20 s) and air-dried for 30 min, as shown in Figure 6A. The polymer-coated filter paper was then placed inside a UV chamber and illuminated with UV light (365 nm, 8 W) to induce cross-linking (Figure 6B). To generate well-defined polymer patterns on the paper surface, black chart paper masks were placed on top of the material during the irradiation step. Next, the polymer-coated filter paper was exposed to the FA vapours. As expected, progressively enhanced fluorescence intensity of filter paper was noticed by the naked eye with increasing FA exposure time (0 to 10 min), and fluorescent colors of test strips gradually changed from light yellow to dark orange under 365 nm UV light (Figure 6C). These results indicate that the designed polymeric probe could serve as a portable paper-based sensor for detecting FA vapours.[38] The vapour phase sensing experiment was carried out at 27 ^{o}C. At this temperature, FA concentration was around 0.1 ppm, so the minimum detection limit in the vapour phase is at 0.1 ppm level [2]. Further studies are in progress to quantify the detection level of FA vapors at different humidity/temperature conditions.

[Insert Figure 6]

3. Conclusions

In conclusion, a naphthalimide-conjugated water-soluble copolymer was designed for FA detection in an aqueous solution through fluorimetric analysis. The solution phase fluorescence "turn-on" of **DCP5** was attributed to the formation **DCP5**-FA adduct through Schiff base reaction, in which the "turn-on" fluorescence mechanism operating through the suppression of PET process was supported by DFT calculations. **DCP5** showed excellent selectivity and sensitivity toward FA over other analytes in the pH range of 4.5 to 7.4 with a detection limit of 1.36 nM in an aqueous medium. Interestingly, **DCP5** could be regenerated

from the **DCP5**-FA adduct, validating the recyclability and reusability of the polymer. This renders the polymer probe a highly practical and environmentally friendly option for continuous monitoring applications. Preliminary results show that the polymer-based sensor coated on a filter paper could be useful as a point-of-care sensor of FA vapour, wherein the observed visual color change under UV-light exposure could be used as an indicator. Further work is in progress to validate this observation, determine the limits of detection, and demonstrate the usefulness of the method for monitoring FA concentration in ambient air. Thus, the present work not only advances our understanding of the FA sensing mechanism but also paves the way for the development of an effective, efficient, and practical method for the detection of formaldehyde in both the aqueous and vapour phase.

Supporting information. Synthesis and characterization details of NDIST and BPMA, polymers synthesis, photostability study, quantum yield calculation, LOD determination method, and DFT calculation details are provided in supporting information.

Acknowledgements. PD acknowledges financial support from the Scheme for Transformational and Advanced Research in Sciences (STARS), Ministry of Human Resource Development, Government of India [File No.: STARS/APR2019/CS/122/FS]. SR acknowledges the Council of Scientific and Industrial Research (CSIR), Government of India, for the senior research fellowship (SRF). SP acknowledges DST-INSPIRE, Government of India, for SRF fellowship.

References

[1] Tang X, Bai Y, Duong A, et al. Formaldehyde in china: production, consumption, exposure levels, and health effects. Environ. Int. 2009;35:1210-1224.

[2] Salthammer T, Mentese S, Marutzky R. Formaldehyde in the indoor environment. Chem. Rev. 2010;110:2536-2572.

[3] Nielsen GD, Larsen ST, Wolkoff P. Re-evaluation of the WHO (2010) formaldehyde indoor air quality guideline for cancer risk assessment. Arch. Toxicol. 2017;91:35-61.

[4] International Agency for Research on Cancer. IARC classifies formaldehyde as carcinogenic to humans; IARC: Lyon, 2004, 15.

[5] Park HJ, Kim J, Choi N, et al. Nonstoichiometric co-rich $ZnCo_2o_4$ hollow nanospheres for high-performance formaldehyde detection at ppb levels. ACS Appl. Mater. Interfaces. 2016;8:3233-3240.

[6] Reingruber H, Pontel LB, Endogenous formaldehyde scavenges cellular glutathione resulting in redox disruption and cytotoxicity. Curr. Opin. Toxicol. 2018;9:28-34.

[7] Zhang L, Steinmaus C, Eastmond DA, et al. Formaldehyde exposure and leukemia: a new meta-analysis and potential mechanisms. Mutat. Res. Rev. Mutat. Res., 2009;681:150-168.

[8] Obata T. Diabetes and semicarbazide-sensitive amine oxidase (SSAO) activity: a review. Life Sciences. 2006;79:417-422.

[9] Tretyakova NY, Groehler A, Ji S. DNA–Protein cross-links: formation, structural identities, and biological outcomes. Acc. Chem. Res. 2015;48:1631-1644.

[10] Korpan YI, Gonchar MV, Sibirny AA, N. Y. Development of highly selective and stable potentiometric sensors for formaldehyde determination. Biosens. Bioelectron. 2000;15:77-83.

[11] Kato S, Post GC, Bierbaum VM, Koch TH. Chemical ionization mass spectrometric determination of acrolein in human breast cancer cells. Anal. Biochem. 2002;305:251-259.

[12] Yang Y, Hao Y, Huang L, T. H. Chen. Recent advances in electrochemical sensors for formaldehyde. Molecules. 2024;29:327 (1-37).

[13] Tang Y, Kong X, Xu A, et al. Development of a two-photon fluorescent probe for imaging of endogenous formaldehyde in living tissues. Angew. Chem. Int. Ed Engl. 2016;55:3356-3359.

[14] Lu X, Li R, Han B, et al. Fluorescence sensing of formaldehyde and acetaldehyde based on responsive inverse opal photonic crystals: A multiple-application detection platform. ACS Appl. Mater. Interfaces. 2021;13:13792-13801.

[15] Brewer TF, Chang CJ. An aza-cope reactivity-based fluorescent probe for imaging formaldehyde in living cells. J. Am. Chem. Soc. 2015;137:10886-10889.

[16] Bruemmer KJ, Walvoord RR, Brewer TF, et al. Development of a general aza-cope reaction trigger applied to fluorescence imaging of formaldehyde in living cells. J. Am. Chem. Soc. 2017;139:5338-5350.

[17] Zhao X, Ji C, Ma L, et al. An aggregation-induced emission-based “turn-on” fluorescent probe for facile detection of gaseous formaldehyde. ACS Sens. 2018;3:2112-2117.

[18] Chua HM, Hui BYK, Chin KLO, et al. Recent advances in aggregation-induced emission (AIE)-based chemosensors for the detection of organic small molecules. Mater. Chem. Front. 2023;7:5561-5660.
[19] Bauri K, Saha B, Mahanti J, De P. A nonconjugated macromolecular luminogen for speedy, selective and sensitive detection of picric acid in water. Polym. Chem. 2017;8:7180-7187.
[20] Pan S, Roy S, Choudhury N, et al. From small molecules to polymeric probes: recent advancements of formaldehyde sensors. Sci. Technol. Adv. Mater. 2022;23:49-63.
[21] Liu G, Shegiwal A, Zeng Y, et al. Polymers for fluorescence imaging of formaldehyde in living systems *via* the hantzsch reaction. ACS Macro Lett. 2018;7:1346-1352.
[22] Li P, Zhang D, Zhang Y, et al. Ultrafast and efficient detection of formaldehyde in aqueous solutions using chitosan-based fluorescent polymers. ACS Sens. 2018;3:2394-2401.
[23] Wang L, Liu Z, Li A, et al. Zero-carbon emission chemical method to remove formaldehyde without catalyst by highly porous polymer composites at room temperature. Macromol. Rapid. Commun. 2023;44:2200629(1-9).
[24] Roy S, Pan S, Choudhury N, et al. Water-soluble polymeric probe with tryptophan pendants for formaldehyde sensing. Eur. Poly. J. 2024;215:113241(1-8).
[25] Min Y, Yuan C, Fu D, Liu J. Removal of formaldehyde and its analogues using a hybrid assembly of pyrene-modified hydrazide and rGO: A negative carbon emission and green chemical decomposition. Langmuir 2023;39:10692-10700.
[26] Hodul JN, Carneiro NF, Murray AK, et al. Poly (5-carboxyindole)–*β*-cyclodextrin composite material for enhanced formaldehyde gas sensing. J. Mater. Sci. 2022;57:11460-11474.
[27] Lu W, Zhang J, Huang Y, et al. Self-diffusion driven ultrafast detection of ppm-level nitroaromatic pollutants in aqueous media using a hydrophilic fluorescent paper sensor. ACS Appl. Mater. Interfaces, 2017;9:23884-23893.
[28] Chung PR, Tzeng CT, Ke MT, Lee CY. Formaldehyde gas sensors: a review. Sensors. 2013;13:4468-4484.
[29] Zhu Y, Li H, Zheng Q, Xu J, Li X. Amine-functionalized SBA-15 with uniform morphology and well-defined mesostructure for highly sensitive chemosensors to detect formaldehyde vapor. Langmuir. 2012;28:7843-7850.
[30] Kim HN, Guo Z, Zhu W, et al. Recent progress on polymer-based fluorescent and colorimetric chemosensors. Chem. Soc. Rev. 2011;40:79-93.

[31] Böhm A, Trosien S, Avrutina O, Kolmar H, Biesalski M. Covalent attachment of enzymes to paper fibers for paper-based analytical devices. Front. Chem. 2018;6:214 (1-10).
[32] Paul S, Ghosh S, Kumar M, et al. Water-soluble napthalimide-conjugated n-nitrosamine-based block copolymers for photoinduced nitric oxide delivery and cell imaging. ACS Appl. Polym. Mater. 2024;6:1075-1085.
[33] Hidayah N, Purwono B, Nurohmah BA, Pranowo HD. A Turn-off fluorescent chemosensor for detecting formaldehyde based on pyridine derivative. Indones. J. Chem. 2019;19:1074 (1-7).
[34] Zhu B, Gao C, Zhao Y, Liu C, et al. A 4-hydroxynaphthalimide-derived ratiometric fluorescent chemodosimeter for imaging palladium in living cells. Chem. Commun. 2011;47:8656-8658.
[35] Tang Y, Kong X, Xu A, et al. Development of a two-photon fluorescent probe for imaging of endogenous formaldehyde in living tissues. Angew. Chem. Int. Ed Engl. 2016;55:3356-3359.
[36] Hileman B. Formaldehyde: assessing the risk. Environ. Sci. Technol. 1984;18:216-221.
[37] Bi A, Gao T, Cao X, et al. A novel naphthalimide-based probe for ultrafast, highly selective and sensitive detection of formaldehyde. Sens. Actuators B Chem. 2018;255:3292-3297.
[38] Zhang F, Chi H, Dong X, et al. Fabrication of an amino functionalized paper-based material for highly efficient detection and adsorption of formaldehyde. ACS Sens. 2024;9:4767-4776.

A naphthalimide-conjugated fluorescent water-soluble polymeric probe is reported for formaldehyde sensing in an aqueous (nanomolar level) phase within a very short time (1 min) with high selectivity. Also, this work demonstrates a facile approach for FA vapor sensing through changes in fluorescence intensity.

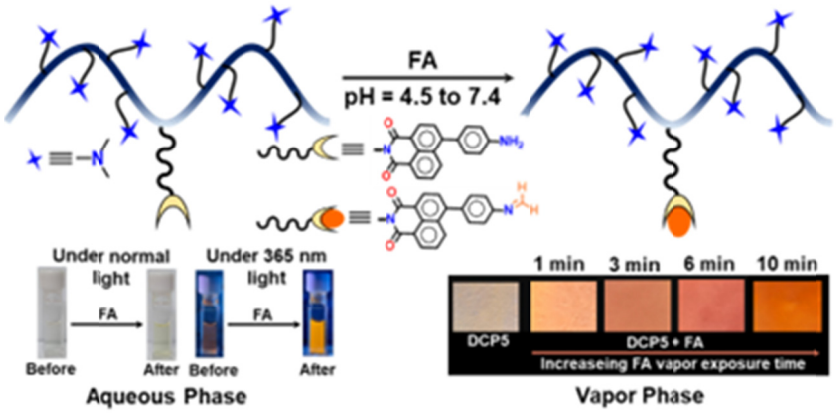

Graphic Abstract

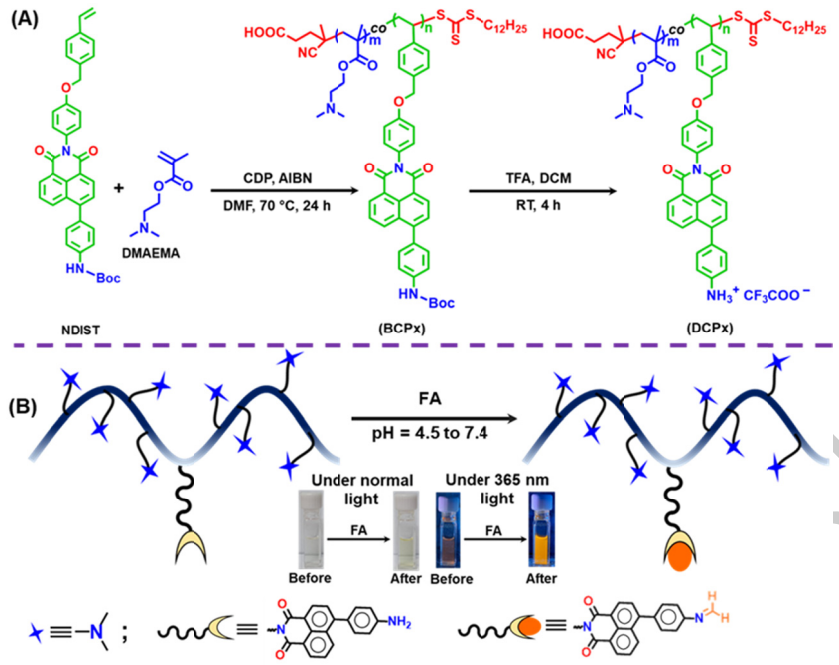

Scheme 1. (A) Synthetic route for the preparation of naphthalimide-conjugated polymeric probe. (B) Schematic representation of FA sensing mechanism with the naphthalimide-conjugated polymeric probe.

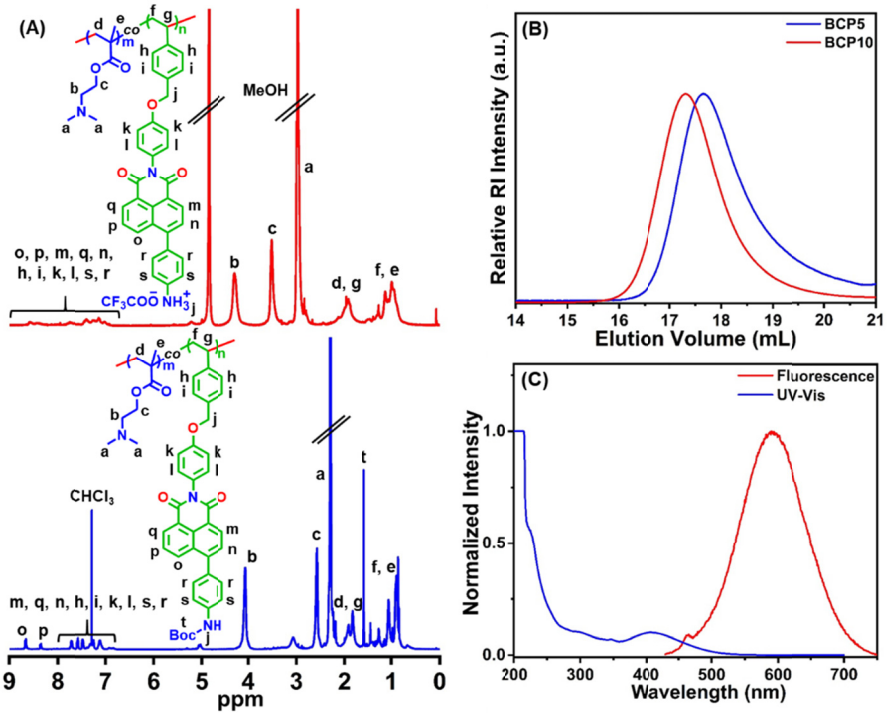

Figure 1. (A) ^{1}H NMR spectra of **BCP5** recorded in $CDCl_3$ (bottom) and **DCP5** recorded in MeOH-d_4 (top). (B) SEC refractive index (RI) traces of BCP5 and BCP10 were recorded in DMF at 40 °C. (C) Normalized UV-Vis and fluorescence spectra of deprotected copolymer (0.25 mg/mL aqueous solution of **DCP5)**.

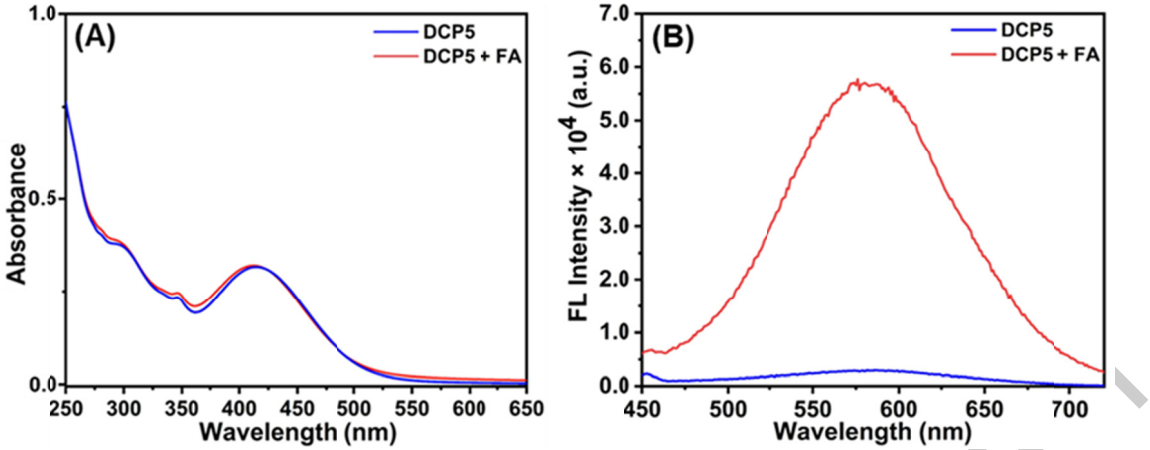

Figure 2. (A) UV-Vis and (B) fluorescence spectra of aqueous **DCP5** solutions (0.25 mg/mL) in the absence and presence of 100 nM of FA.

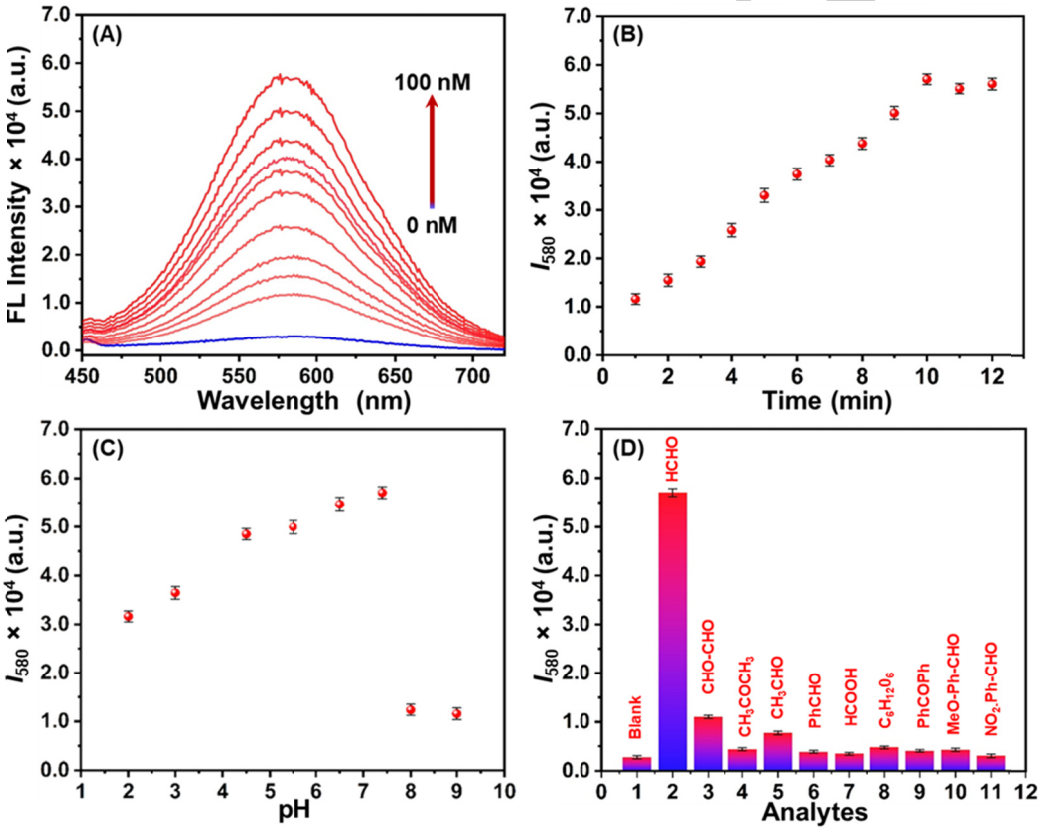

Figure 3. (A) The emission spectra of **DCP5** solutions (0.25 mg/mL) in the presence of various concentrations of FA, measured 1 min after FA addition. (B) Time-dependent emission intensity change of **DCP5** solutions at 580 nm with 100 nM of FA. (C) Fluorescence intensity of the aqueous **DCP5** solutions (0.25 mg/mL) at different pH levels after reaction with 100 nM FA. (D) Bar graph illustrating the emission intensities of **DCP5** (0.25 mg/mL) at 580 nm in the presence of FA and other analytes (measured after 10 min).

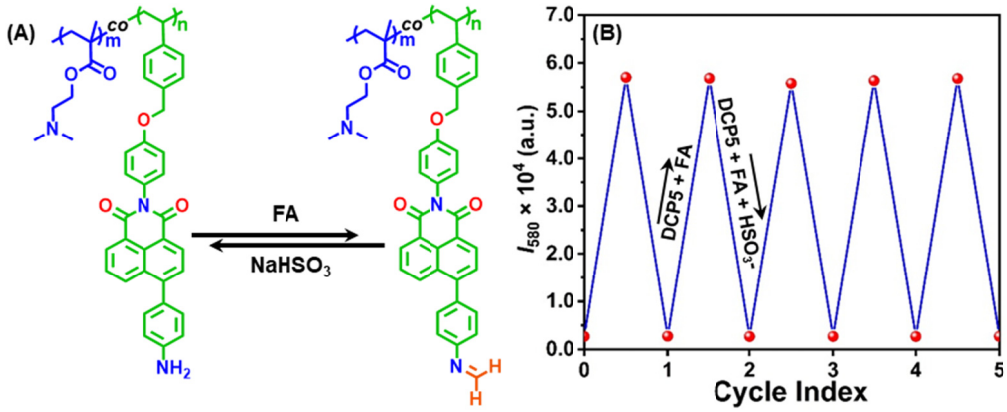

Figure 4. (A) Sensing mechanism of the **DCP5** polymeric probe for FA/bisulfite. (B) Reversibility study of **DCP5** between FA and bisulfite.

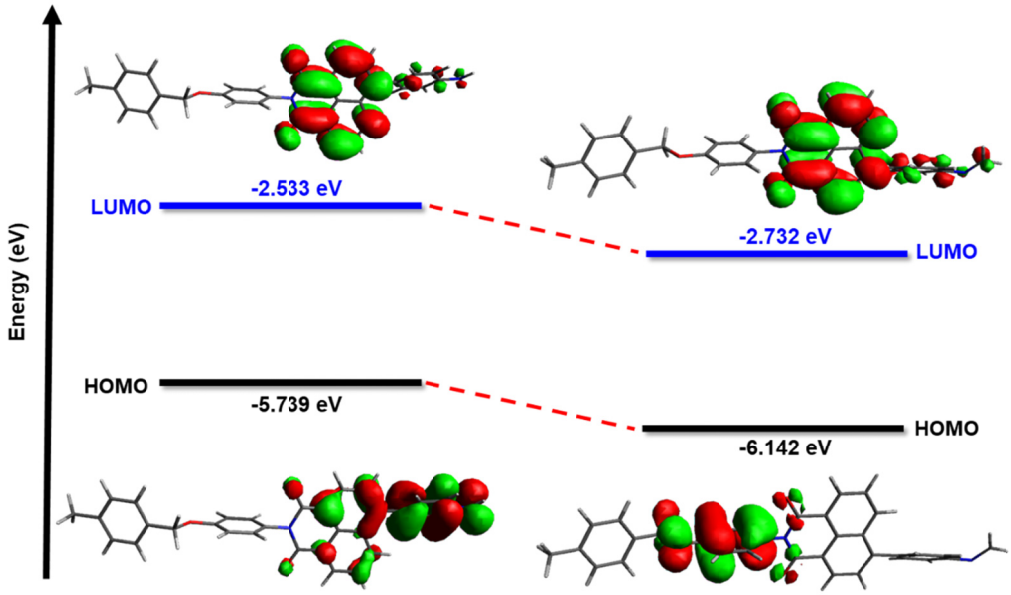

Figure 5. HOMO-LUMO energy difference of the NDIST repeating unit before and after adding FA, calculated using DFT with the B3LYP/6-311G(d) basis set.

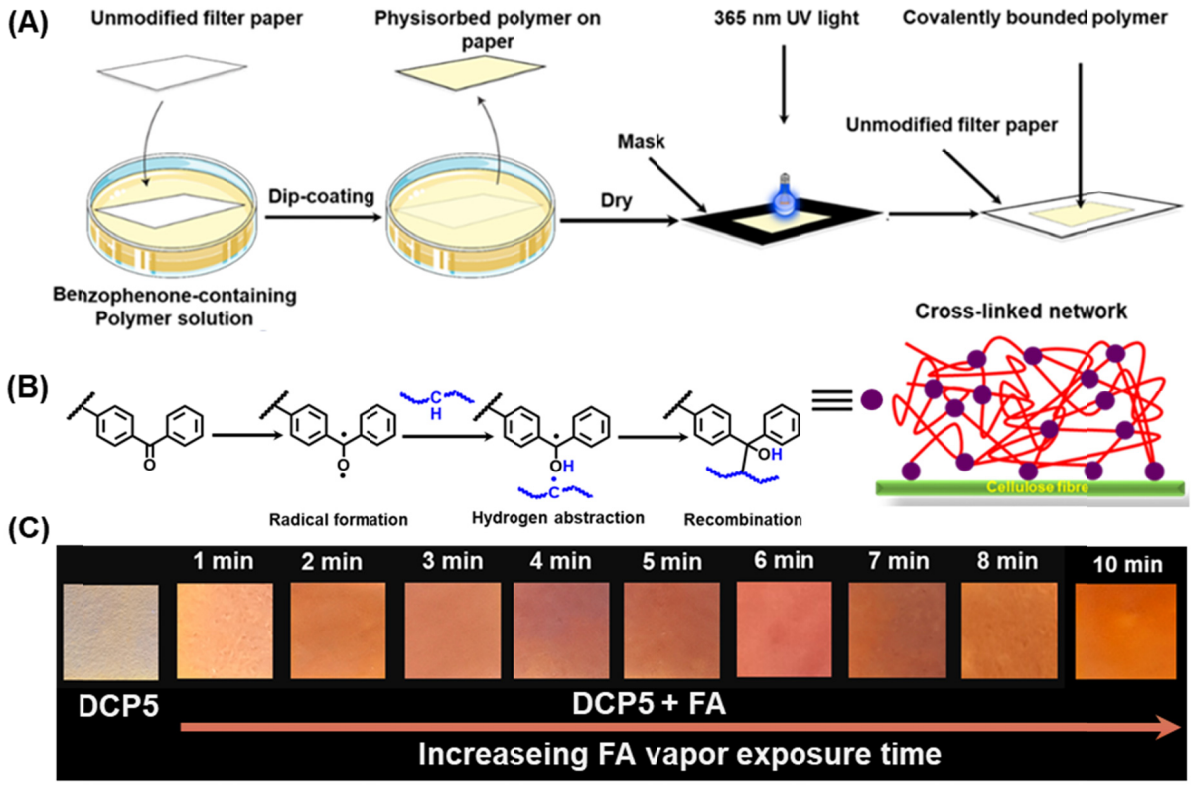

Figure 6. UV-light induced immobilization of benzophenone-containing polymer on the filter paper. (A) General procedure for cross-linking using carbon chart mask. (B) Probable mechanism of light-induced cross-linking of benzophenone moieties. (C) Photographs of **DCP5** coated paper strip before and after the exposure to FA vapor.

A naphthalimide-conjugated fluorescent water-soluble polymeric probe is reported for formaldehyde sensing in an aqueous (nanomolar level) phase within a very short time (1 min) with high selectivity. Also, this work demonstrates a facile approach for FA vapor sensing through changes in fluorescence intensity.

Supporting Information for

Naphthalimide-based fluorescent polymeric probe: A dual-phase sensor for formaldehyde detection

Subhadip Roy,[1] Swagata Pan,[1] Swaminathan Sivaram[2,*] and Priyadarsi De[1,*]

[1]Polymer Research Centre and Centre for Advanced Functional Materials, Department of Chemical Sciences, Indian Institute of Science Education and Research Kolkata, Mohanpur-741246, Nadia, West Bengal, India.

[2]Indian Institute of Science Education and Research Pune, Dr. Homi Bhabha Road, Pune - 411008, India.

*Corresponding authors: emails: s.sivaram@iiserpune.ac.in (SS); p_de@iiserkol.ac.in (PD)

Experimental section

Materials. 2-(Dimethylamino)ethyl methacrylate (DMAEMA), 4-vinyl benzyl chloride (4-VBC), 4-aminophenol, sodium *tert*-butoxide (NaO^{t}Bu), *N*,*N*-dimethylformamide (DMF, 99.9%), formaldehyde (FA, HCHO, 37% in water), phosphate buffered saline (PBS), and di-*tert*-butyl dicarbamate ($(Boc)_2O$, 98%) were purchased from Sigma Aldrich. 4-Bromo-1,8-naphthalic anhydride (95%) and palladium-tetrakis(triphenylphosphine) ($Pd(PPh_3)_4$) were bought from BLD *Pharmatech Ltd*. India. The 2,2′-azobis(isobutyronitrile) (AIBN, 98%, SRL, India) was recrystallized from methanol and used as an initiator during the polymerization. 4-Cyano-(dodecylsulfanylthiocarbonyl)sulfanylpentanoic acid (CDP) was prepared following previous standard literature [1]. Benzophenone-based monomer (BPMA) was prepared following a previous literature procedure [2]. Dialysis membrane with molecular weight cutoff (MWCO) = 6000-8000 g/mol (Spectra/Por®, diameter 14.6 mm, flat width 23 mm, volume/length 1.7 mL/cm) was purchased from Spectrum Laboratories, USA. The NMR solvents $CDCl_3$ (99.8% D), MeOH-d_4, and DMSO-d_6 (99% D) were purchased from Cambridge Isotope Laboratories, Inc., USA. Dichloromethane (DCM), chloroform ($CHCl_3$), hexane (a mixture of isomers), acetone, methanol (MeOH), ethanol (EtOH), ethyl acetate (EtOAc), trifluoro acetic acid (TFA), diethyl ether, tetrahydrofuran (THF), dimethyl sulfoxide (DMSO), acetonitrile (MeCN), HPLC graded water, potassium carbonate (K_2CO_3), sodium sulfate (Na_2SO_4), sodium bicarbonate ($NaHCO_3$), and hydrochloric acid (HCl) were

obtained from Merck, India. THF, hexane, DCM, acetone, EtOAc, and MeOH were purified by following standard protocols [3].

Instruments and characterizations

Nuclear magnetic resonance (NMR). ^{1}H NMR spectroscopic measurements were recorded in either 500 MHz Bruker AvanceIII NMR spectrometer or 400 MHz JEOL ECS NMR spectrometer at 25 °C using tetramethylsilane (TMS) as an internal reference. MeOH-d_4, DMSO-d_6, and $CDCl_3$ were used as solvents to record the spectra depending on the solubility of the compounds.

Electrospray ionization mass spectrometry (ESI-MS). The ESI-MS spectra were measured in Waters Xevo® G2-XS QTof mass spectrometer using positive mode and negative mode electrospray ionization. 1.0 mM concentration of the compounds was prepared in MeCN or MeOH. The solution was filtered *via* a polytetrafluoroethylene (PTFE) syringe filter (0.45 μm) before the experiment.

UV-Vis spectroscopy. UV-Vis spectra of the polymers were recorded in a PerkinElmer Lambda 35 spectrophotometer.

Fluorescence spectroscopy. The emission spectra of the polymers were measured in a Horiba JobinYvon fluorescence spectrometer (Fluoromax-3, Xe-150 W, 250-900 nm).

Size exclusion chromatography (SEC). The number average molar mass ($M_{n,SEC}$) and dispersity ($Đ$) of the polymers were determined using SEC in DMF with 0.8 mL/min flow rate at 40 °C. The instrument contains a Waters 1515 HPLC pump, a Waters 2414 refractive index (RI) detector, two PolarGel-M analytical columns (300 × 7.5 mm), and one PolarGel-M guard column (50 × 7.5 mm). The calibration curve of the instrument was prepared using poly(methyl methacrylate) (PMMA) standards from Agilent technologies. Typically, the polymers were dissolved in DMF (1 mg/mL) and passed through a 0.45 μm PTFE syringe filter before the experiment.

Attenuated total reflection Fourier transform infrared spectroscopy (ATR-FTIR). ATR-FTIR spectroscopy was used to record the bond stretching frequency of samples in the solid state using a Bruker Alpha Platinum-ATR instrument.

Synthesis of 4-((4-vinylbenzyl)oxy)aniline (C1). The **C1** was synthesized following the previous literature [4]. Typically, 4-aminophenol (2.5 g, 20.8 mmol) was taken in a 250 mL round-bottom flask and dissolved in 65 mL of DMF. Then, NaO^{t}Bu (2.2 g, 22.8 mmol) was added to the solution, and after 5 min the flask was kept at 90 ℃. 4-Vinyl benzyl chloride (3.2 g, 20.8 mmol) was added dropwise to the reaction mixture after 10 min of stirring. The completion of the reaction was monitored by thin-layer chromatography. Next, the solution was diluted with 500 mL of DCM. This organic layer was washed with ice-cold water (4 × 200 mL) and brine solution (200 mL). The organic layer was collected and dried over anhydrous Na_2SO_4 and purified the compound by column chromatography with 20-25% (v/v) EtOAc in hexane mixture. Yield = 70%. **C1** was characterized using ^{1}H NMR spectroscopy. ^{1}H NMR (400 MHz, $CDCl_3$, δ ppm): 7.40 (q, J = 8.2 Hz, 4H), 6.84–6.78 (m, 2H), 6.72 (d, J = 17.6 Hz, 1H), 6.67–6.60 (m, 2H), 5.76 (d, J = 17.6 Hz, 1H), 5.25 (d, J = 10.9 Hz, 1H), 4.98 (s, 2H), 3.46 (broad, 2H).

Synthesis of 6-bromo-2-(4-((4-vinylbenzyl)oxy)phenyl)-1H-benzo[de]isoquinoline-1,3(2H)-dione (C2). 4-bromo-1,8-naphthalic anhydride (2.4 g, 8.9 mmol) was taken in a 100 mL round-bottom flask and 50 mL of EtOH was added. The flask was kept at 70 ℃ and Et_3N (1.8 g, 8.9 mmol) was added to the solution. After 15 min of stirring, **C1** (2.0 g, 8.9 mmol) was added to the reaction mixture. The reaction condition was maintained overnight, resulting in the formation of a white precipitate. The reaction mixture was then cooled and the precipitate was filtered and washed with EtOH. The white color compound was dried under vacuum at 45 ℃ overnight. Yield = 75%. **C2** was characterized by ^{1}H NMR analysis. ^{1}H NMR (500 MHz, DMSO-d_6, δ ppm): 8.56 (dd, J = 10.4, 7.8 Hz, 2H), 8.30 (d, J = 7.9 Hz, 1H), 8.22 (d, J = 7.9 Hz, 1H), 8.06–7.95 (m, 1H), 7.53–7.40 (m, 4H), 7.26 (d, J = 9.0 Hz, 2H), 7.10 (d, J = 8.8 Hz, 2H), 6.73 (dd, J = 17.7, 11.0 Hz, 1H), 5.82 (d, J = 17.7 Hz, 1H), 5.25 (d, J = 10.9 Hz, 1H), 5.14 (s, 2H).

Synthesis of 6-(4-aminophenyl)-2-(4-((4-vinylbenzyl)oxy)phenyl)-1H-benzo[de]isoquinoline-1,3(2H)-dione (C3). C2 (500.0 mg, 1.1 mmol), 4-amino boronic acid (215.4 mg, 1.2 mmol), and K_2CO_3 (286.1 mg, 2.1 mmol) were taken in a sealed tube. Next, 7 mL DMF and 2 mL water were added and purged with dry N_2 for 10 min. After that, $Pd(PPh_3)_4$ (60.0 mg, 51.0 μmol) was added to the reaction mixture. The sealed tube was then placed on a preheated oil bath at 90 ℃ for 18 h. After completion of the reaction, the solution was diluted with 200 mL of DCM. This organic layer was washed with ice water (5 × 200

mL) and brine solution (200 mL). The organic layer was passed through anhydrous Na_2SO_4 and purified by column chromatography with 50-60% (v/v) EtOAc in hexane mixture. Yield = 65%. **C3** was characterized by ^{1}H NMR and ESI-MS spectroscopy. ^{1}H NMR (500 MHz, DMSO-d_6, δ ppm): 8.56 – 8.42 (m, 3H), 7.87 (dd, J = 5.1, 4.3 Hz, 1H), 7.75 (d, J = 4.6 Hz, 1H), 7.57 – 7.45 (m, 4H), 7.30 (dd, J = 5.2, 1.9 Hz, 4H), 7.15 (d, J = 5.4 Hz, 2H), 6.81 – 6.76 (m, 3H), 5.87 (d, J = 10.6, 0.8 Hz, 1H), 5.54 (s, 2H), 5.30 (dd, J = 6.5, 0.6 Hz, 1H), 5.19 (s, 2H). Mass (*m/z*) calculated for $C_{33}H_{24}N_2O_3$ $[M + H]^+$ = 497.1820; observed = 497.1848.

Synthesis of *tert*-butyl (4-(1,3-dioxo-2-(4-((4-vinylbenzyl)oxy)phenyl)-2,3-dihydro-1H-benzo[de]isoquinolin-6-yl)phenyl)carbamate (NDIST). C3 (500.0 mg, 0.8 mmol) was taken in a 250 mL round-bottom flask and dissolved in 75 mL dioxane equipped with a magnetic stir bar. The reaction mixture was then placed in an ice-water bath and di-*tert*-butyl dicarbamate (0.8 mmol) was added dropwise into the reaction mixture. The reaction was continued to stir for 24 h. After completion of the reaction, the solution was diluted with 300 mL of DCM. This organic layer was washed with water (5 × 200 mL) and brine solution (200 mL). The organic layer was dried over anhydrous Na_2SO_4 and purified using column chromatography with 30% (v/v) EtOAc in hexane mixture. Yield = 45%. NDIST was characterized by ^{1}H NMR and ESI-MS analysis. ^{1}H NMR (500 MHz, DMSO-d_6, δ ppm): 9.65 (s, 1H), 8.58 – 8.47 (m, 2H), 8.36 (d, J = 5.1 Hz, 1H), 7.88 (d, J = 5.1 Hz, 1H), 7.81 (d, J = 4.5 Hz, 1H), 7.71 (d, J = 5.2 Hz, 2H), 7.59 – 7.43 (m, 6H), 7.31 (d, J = 5.3 Hz, 2H), 7.15 (d, J = 5.4 Hz, 2H), 6.77 (d, J = 10.6 Hz, 1H), 5.87 (d, J = 10.6 Hz, 1H) 5.29 (d, J = 6.5, Hz, 1H), 5.19 (s, 2H), 1.53 (s, 9H). ^{13}C NMR (126 MHz, DMSO-d_6, δ ppm): 162.59, 163.74, 157.18, 150.92, 138.88, 137.21, 137.18, 136.79, 134.44, 131.27, 130.61, 130.27, 129.61, 128.76, 129.00, 128.49, 128.45, 127.49, 127.39, 126.71, 124.60, 122.94, 120.86, 115.30, 118.94, 108.99, 105.06, 70.64, 45.39 35.65. Mass (*m/z*) calculated for $C_{38}H_{32}N_2O_5$ $[M + H]^+$ = 597.2311; observed = 597.2307.

Synthesis of BCP5 and BCP10 copolymers. A typical procedure for the reversible addition-fragmentation chain transfer (RAFT) polymerization technique was followed [5]. For example, **BCP5** (Table **S1**) was synthesized by taking DMAEMA (250.0 mg, 1.6 mmol), NDIST (50. 0 mg, 83.8 μmol), CDP (6.8 mg, 16.8 μmol), AIBN (0.6 mg, 3.7 μmol, from a stock solution of AIBN in DMF), and 1.2 mL DMF in a 20 mL polymerization vial equipped with a magnetic stir bar. Next, the polymerization vial was purged with N_2 for 10 min and placed in a preheated block at 70 °C for 24 h. The polymerization process was quenched by

immersing the vial in ice-water bath and exposing it to air. The resultant copolymer was precipitated in cold hexane, then dissolved in acetone and reprecipitated (4 times) from hexane. The polymers were purified by dialyzing against methanol using a membrane with a molecular weight cutoff (MWCO) of 6000-8000 Da. The methanol was replaced every 2 to 6 h for at least 5 times. The polymer was dried under vacuum for 12 h at 40 °C to obtain a yellow solid powder. Additionally, another copolymer, **BCP10**, was prepared following a similar procedure by varying the feed ratio of DMAEMA and NDIST.

Boc groups deprotection from polymers. The Boc groups of the copolymers were deprotected by using TFA in DCM at room temperature. Typically, in a 20 mL glass vial containing a small magnetic stir bar, 500 mg of copolymer was dissolved in 1 mL DCM. After that, 2.0 mL of TFA was dropwise added to the polymer solution and stirred for 4 h at room temperature. The polymer was then purified by precipitating in diethyl ether. The desired deprotected copolymer was dried in vacuum for 12 h to obtain an orange powder. The Boc group deprotected **BCP5** and **BCP10** were named as **DCP5** and **DCP10**, respectively.

Limit of detection (LOD) determination. Fluorescence titration measurements were carried out to determine the LOD value of **DCP5**. 1.0 mg/mL solution of **DCP5** was prepared in phosphate buffer saline (PBS) as a stock solution. Formaldehyde (FA) stock solution was prepared in Milli-Q water (freshly prepared by diluting 3.7 µL of commercial 37 wt. % FA solution in 500 µL of Milli-Q water). Different concentrations of FA (10-100 nM) were added to the **DCP5** solution and the fluorescence intensities were measured at 580 nm (excitation wavelength, λ_{ex} = 420 nm). The experiment was three times repeated to determine the standard deviation (σ) of the blank polymer samples. The LOD value was calculated using equation (1), following a well-established literature protocol [6].

$$\mathrm{LOD} = \frac{3\sigma}{K} \qquad (1)$$

where K represents the calibration curve slope at low FA concentrations, and σ denotes the standard deviation of the emission intensity for the blank polymer solution. The calculated LOD was 1.36 nM while, K = 4975 and σ = 2260.

Density functional theory (DFT) calculation. The geometry of the naphthalimide-conjugated repeating unit in the deprotected copolymer and the corresponding imine after the reaction with FA *via* addition-elimination reaction were optimized by DFT calculations. The

calculations were evaluated with B3LYP functional and 6-311G as basis set using Gaussian 09 [7].

Quantum yields measurements. Absolute quantum yields were measured *via* an integrating sphere (Xe-400 lamp and PMT-900 + integrating sphere detector) method from Edinburgh Instruments.

Synthesis of the benzophenone-based copolymers (P(DMAEMA-*co*-NDIST-*co*-BPMA)). DMAEMA (383.9 mg, 1.8 mmol), NDIST (81.0 mg, 0.14 mmol), BPMA (36.14 mg, 0.14 mmol), CDP (10.4 mg, 0.03 mmol), and AIBN (0.9 mg, 5.2 μmol, from a stock solution of AIBN in DMF) were dissolved in 2 mL DMF in a 20 mL septum-capped vial. The reaction mixture contains 5% of NDIST and 5% of BPMA, while the molar ratio of [CDP]:[AIBN] was 1:0.2. The solution was purged with N_2 for 10 min and then placed in a preheated block at 70 °C for 24 h. The polymerization reaction was quenched by putting the vial in an ice-water bath and exposed to air. The viscous polymer solution was precipitated in cold hexane. It was dissolved in acetone and reprecipitated (4 times) from hexane. The polymer, P(DMAEMA-*co*-NDIST-*co*-BPMA), was dried under vacuum for 12 h at 40 °C to obtain a yellow solid powder (Scheme **S2**). Monomer conversion was determined as 70% (gravimetric analysis).

Synthesis of P(DMAEMA-*co*-DNDIST-*co*-BPMA). Boc groups in P(DMAEMA-*co*-NDIST-*co*-BPMA) were deprotected using TFA in DCM at room temperature. Typically, in a 20 mL glass vial equipped with a small magnetic stir bar, 200 mg of P(DMAEMA-*co*-NDIST-*co*-BPMA) was dissolved in 0.5 mL DCM and placed in an ice-water bath. Next, 1.0 mL TFA was added dropwise to the solution and the reaction mixture was stirred for 4 h at room temperature. The polymer was purified by precipitation in diethyl ether, and dried under vacuum for 12 h to obtain an orange colored powdered P(DMAEMA-*co*-DNDIST-*co*-BPMA).

General procedure for light-induced immobilization of BPMA-containing polymer. For covalent attachment of P(DMAEMA-*co*-DNDIST-*co*-BPMA) onto a filter paper, the copolymer P(DMAEMA-*co*-DNDIST-*co*-BPMA) was dissolved in MeOH at a concentration of 5 mg/mL. Subsequently, the desired-sized filter papers were soaked in the polymer solution by dip-coating (submerging for 20 s) and air-drying for 30 min. Next, the materials

were exposed to 365 nm UV light for 30 min to induce crosslinking of the polymers. Of note, to generate well-defined polymer patterns on the paper surface, black paper masks were placed on top of the polymer-coated filter paper during the illumination step.

[Insert Scheme S1]

[Insert Figure S1]

[Insert Figure S2]

[Insert Figure S3]

[Insert Figure S4]

[Insert Figure S5]

[Insert Figure S6]

[Insert Table S1]

[Insert Figure S7]

[Insert Figure S8]

[Insert Figure S9]

[Insert Figure S10]

[Insert Figure S11]

[Insert Figure S12]

[Insert Figure S13]

[Insert Figure S14]

[Insert Scheme S2]

References

[1] Moad G, Chong YK, Postma A, et al. Advances in RAFT polymerization: the synthesis of polymers with defined end-groups. Polymer. 2005;46:8458-8468.

[2] Böhm A, Trosien S, Avrutina O, Kolmar H, Biesalski M. Covalent attachment of enzymes to paper fibers for paper-based analytical devices. Front. Chem. 2018;6:214 (1-10).

[3] Furniss BS, Hannaford AJ, Smith PDG, Tatchell AR, in Vogel's Textbook of Practical Organic Chemistry, Longman Scientific & Technical Co-published in the United States with John Wiley & Sons, Inc., New York, 1989.

[4] Paul S, Ghosh S, Kumar M, et al. Water-soluble napthalimide-conjugated n-nitrosamine-based block copolymers for photoinduced nitric oxide delivery and cell imaging. ACS Appl. Polym. Mater. 2024;6:1075-1085.

[5] Das S, Banerjee A, Roy S, et al. Zwitterionic polysulfobetaine inhibits cancer cell migration owing to actin cytoskeleton dynamics. ACS Appl. Bio Mater. 2024, 7, 144-153.

[6] Zhu B, Gao C, Zhao Y, Liu C, et al. A 4-hydroxynaphthalimide-derived ratiometric fluorescent chemodosimeter for imaging palladium in living cells. Chem. Commun. 2011;47:8656-8658.

[7] Frisch MJ, Trucks GW, Schlegel HB, et al. In Gaussian 09, Gaussian, Inc, Wallingford, CT, USA, 2009.

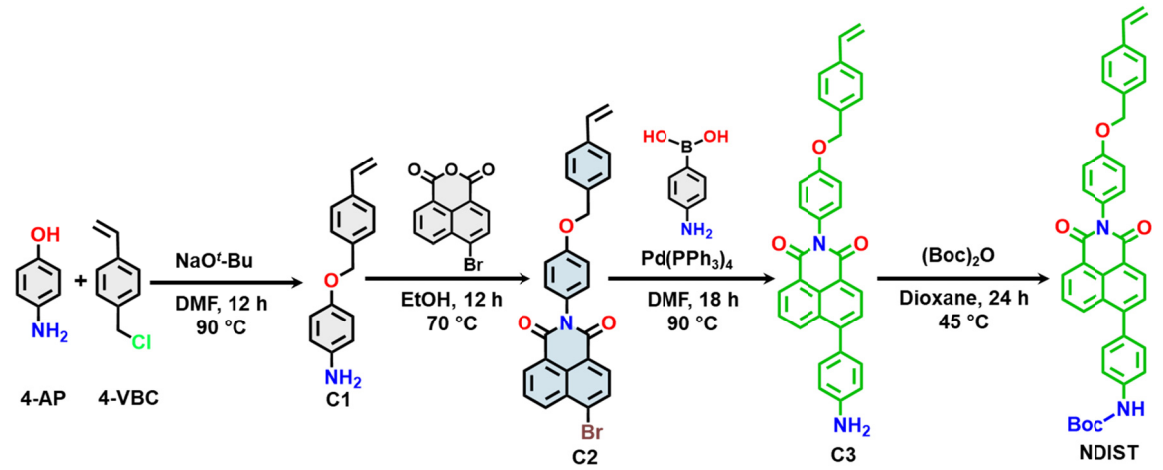

Scheme S1. Synthetic scheme for the monomer.

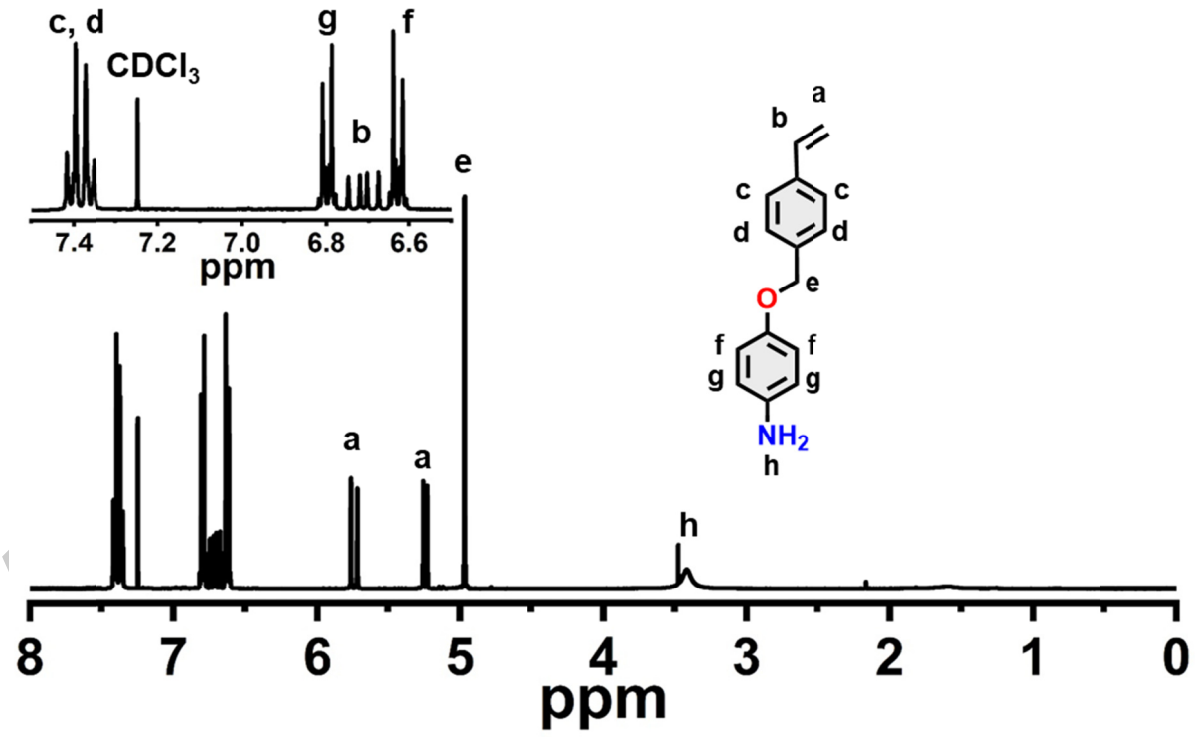

Figure S1. ^{1}H NMR spectrum of **C1** recorded in $CDCl_3$.

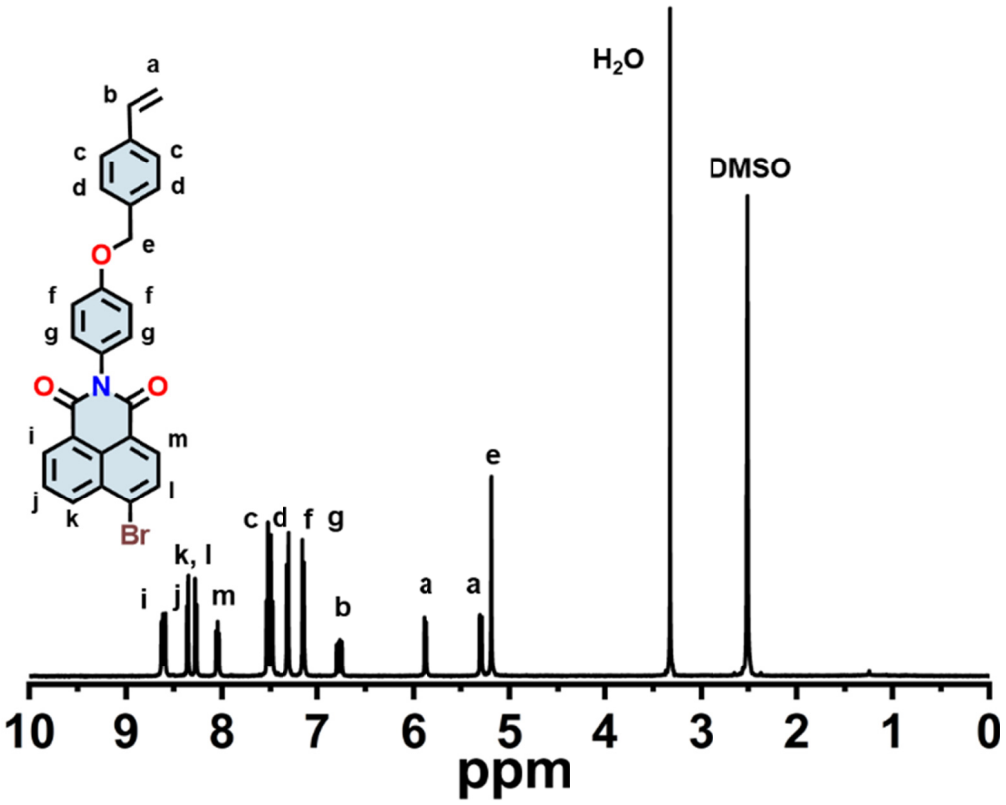

Figure S2. ^{1}H NMR spectrum of **C2** recorded in DMSO-d_6.

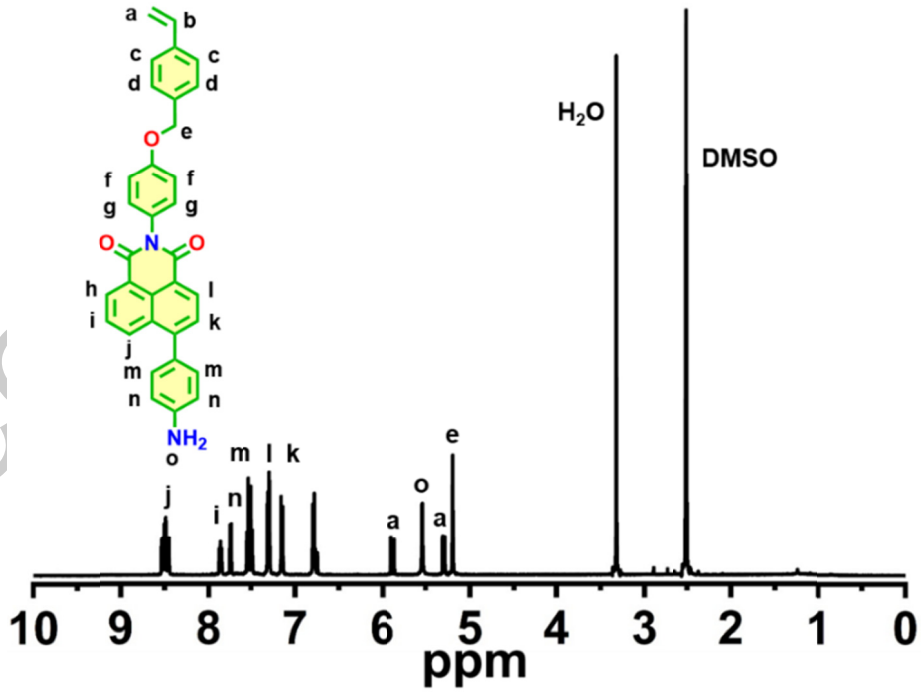

Figure S3. ^{1}H NMR spectrum of **C3** in DMSO-d_6.

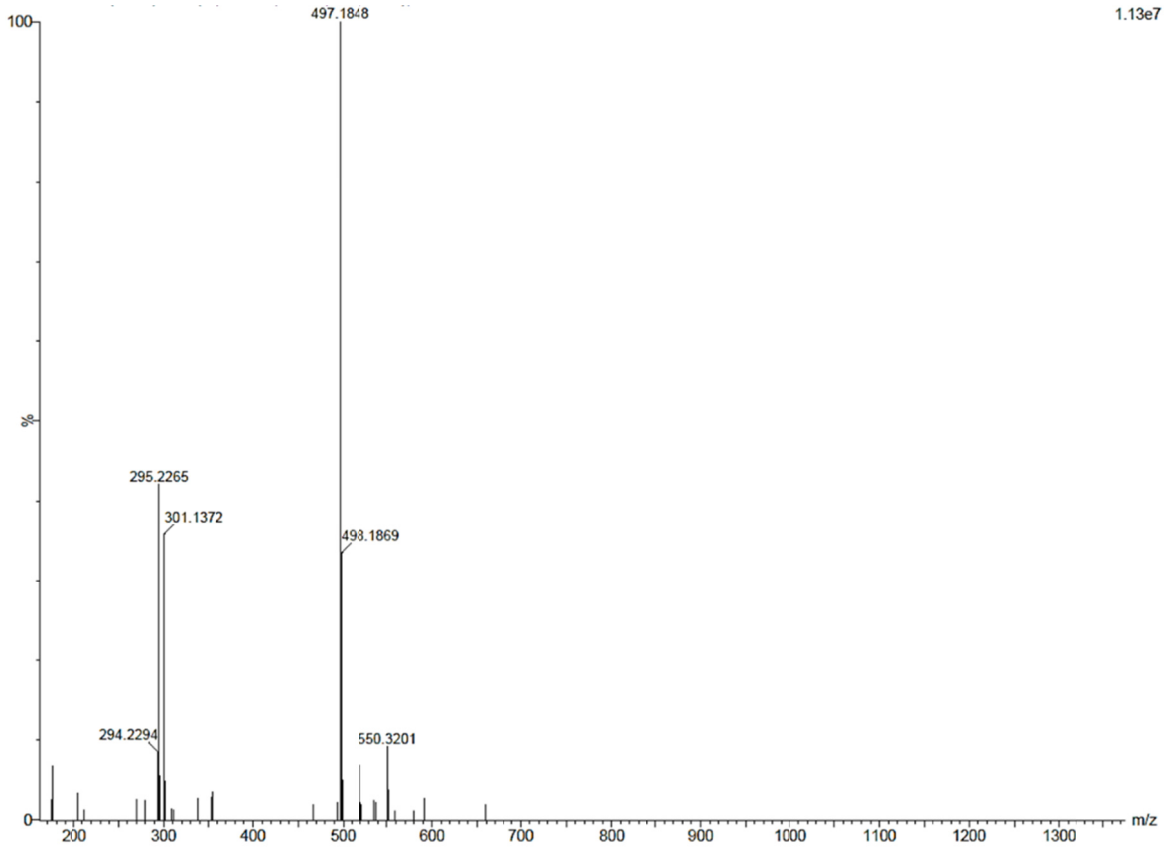

Figure S4. ESI-MS spectrum of **C3**. Mass (*m/z*) calculated for $C_{33}H_{24}N_2O_3$ $[M + H]^+$ = 497.1820; observed = 497.1848.

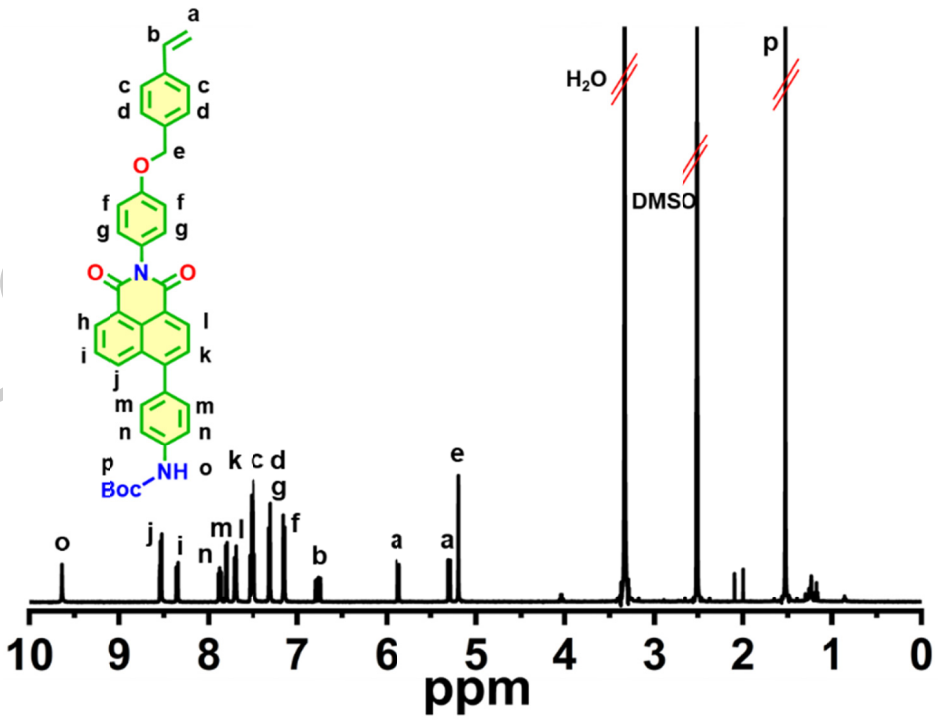

Figure S5. ^{1}H NMR spectrum of **NDIST** in DMSO-d_6.

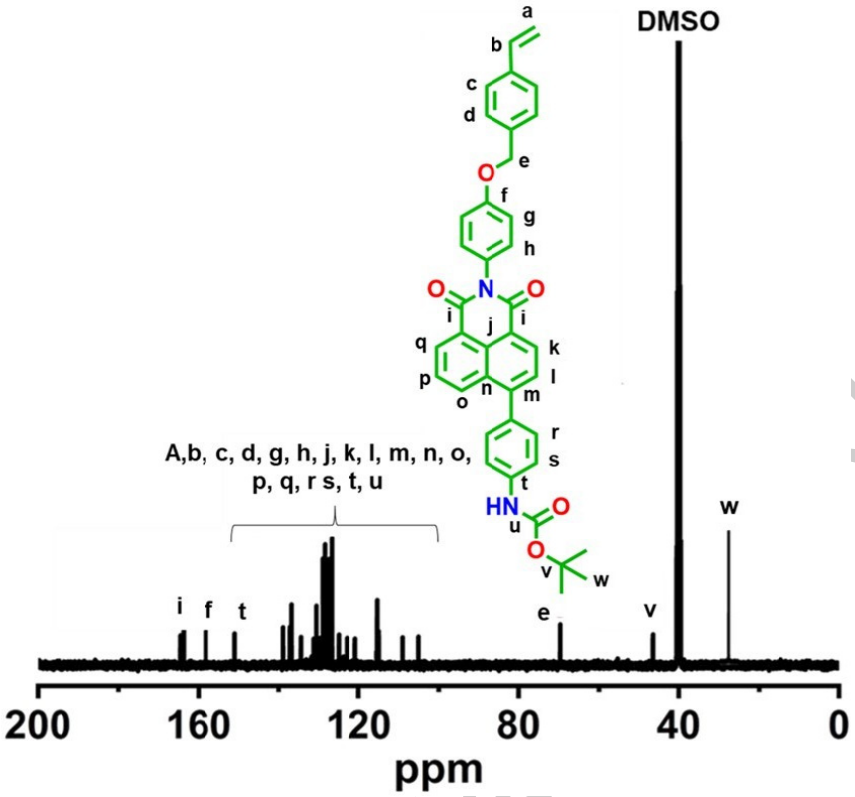

Figure S6. ^{13}C NMR spectrum of **NDIST** in DMSO-d_6.

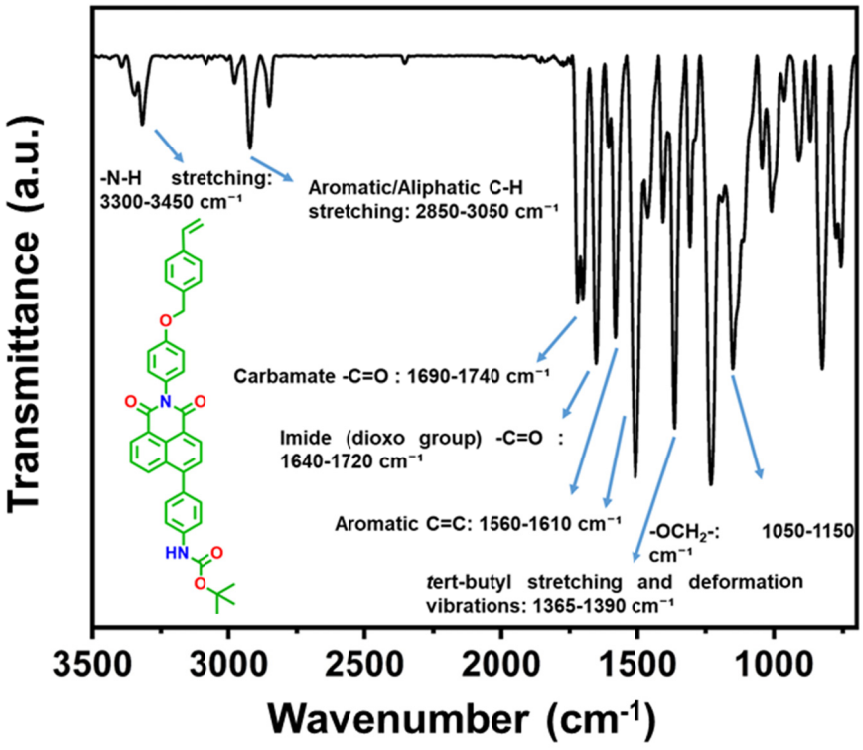

Figure S7. ATR-FTIR spectrum of monomer **NDIST**.

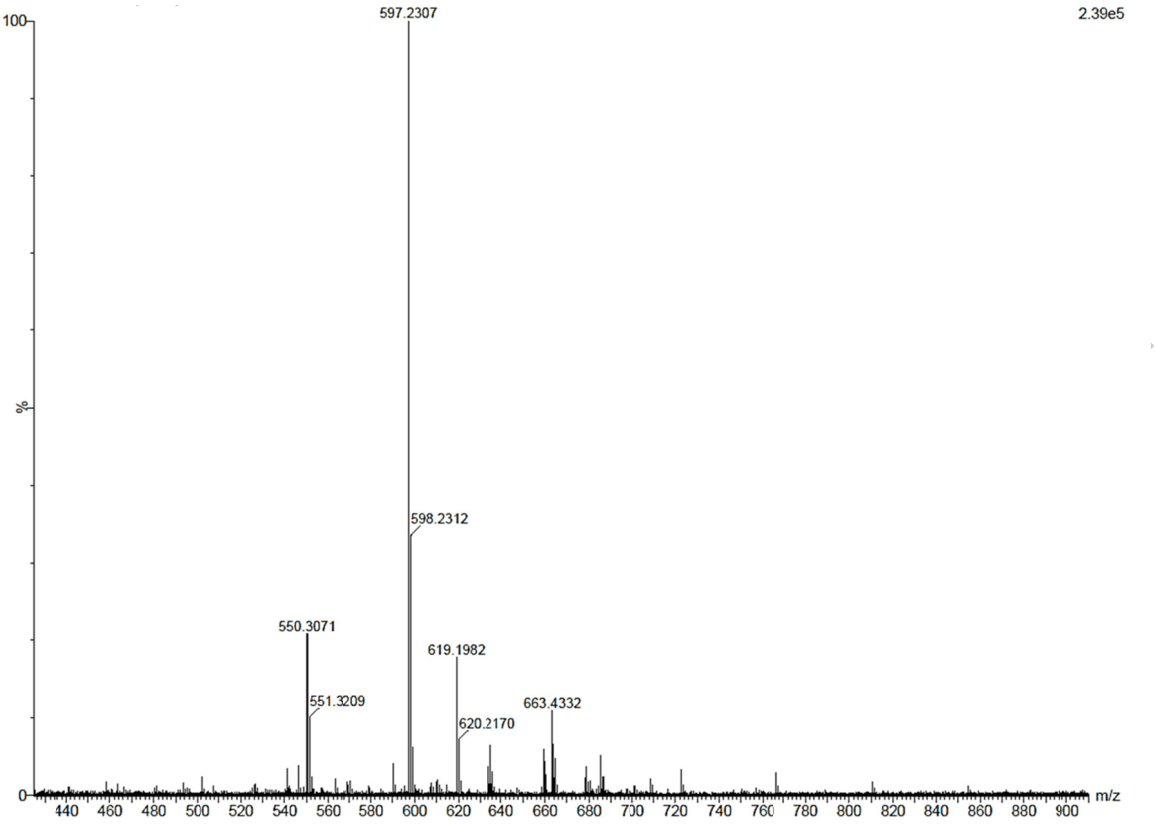

Figure S8. ESI-MS spectrum of NDIST. Mass (*m/z*) calculated for $C_{38}H_{32}N_2O_5$ $[M + H]^+$ = 597.2311; observed = 597.2307.

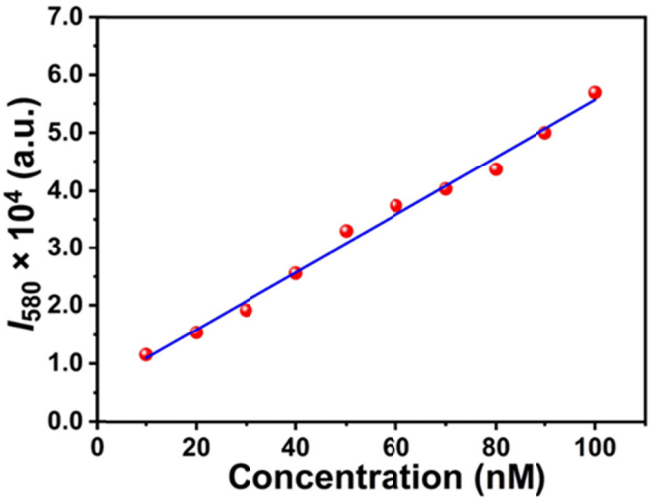

Figure S9. LOD calculation plot of **DCP5** in PBS.

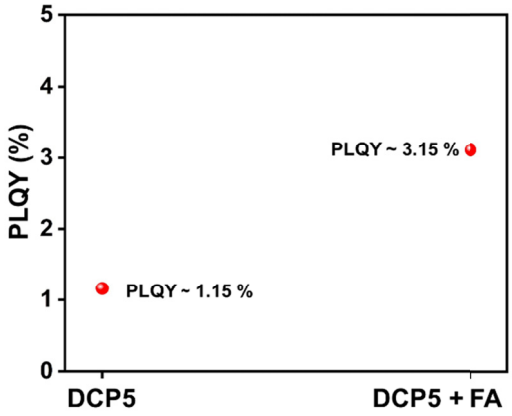

Figure S10. Photoluminescence quantum yield (PLQY) before and after formaldehyde addition to **DCP5** polymer in aqueous phase.

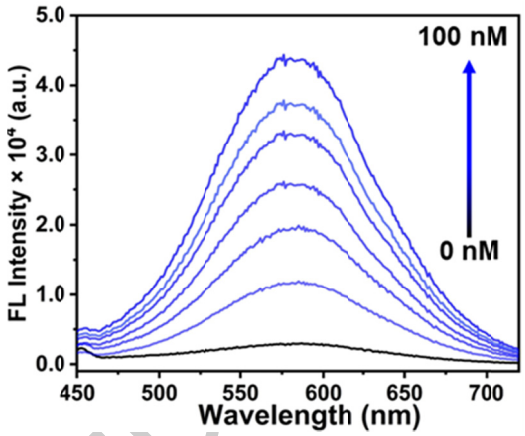

Figure S11. The emission spectra of **C3** in a DMSO/H_2O mixture (2:8, v/v) (10^{-4} M) in the presence of various concentrations of FA (10 to 100 nM). Spectra were measured after 1 min after the FA addition.

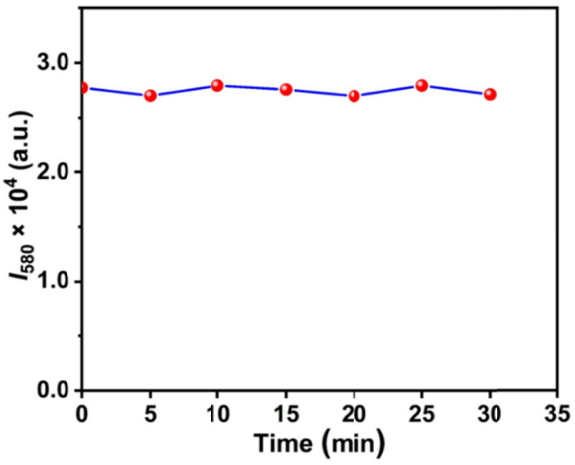

Figure S12. Photostability of the polymeric probe (**DCP5**) at 580 nm emission intensity (irradiation at 420 nm).

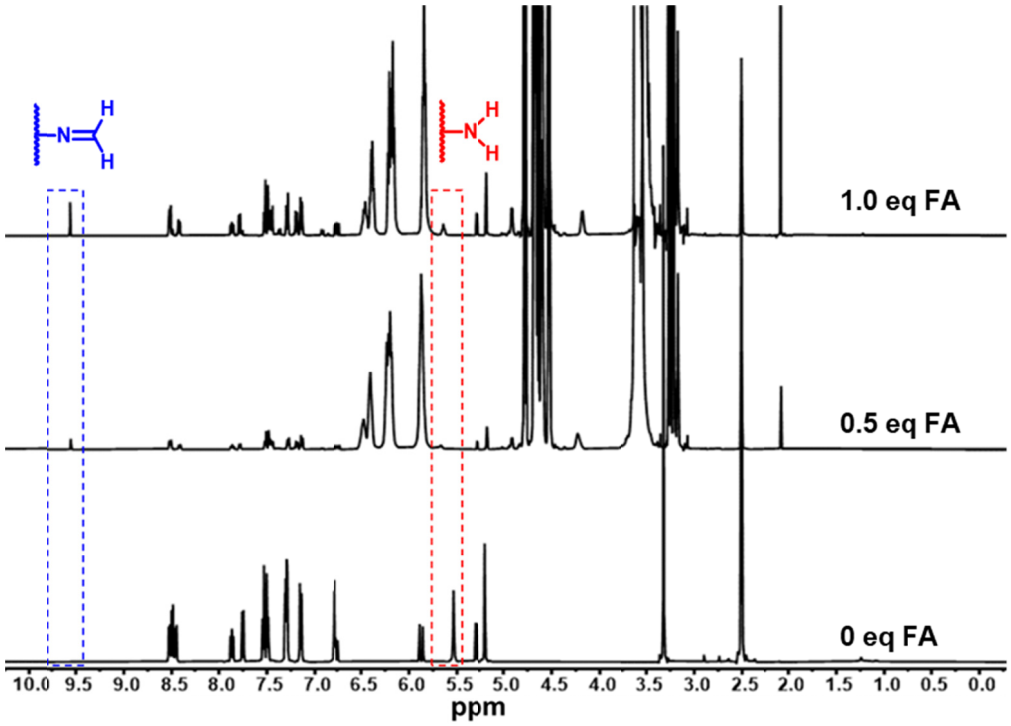

Figure S13. ^{1}H NMR titration spectra in DMSO-d_6 of the model compound **C3** with the increasing FA concentrations.

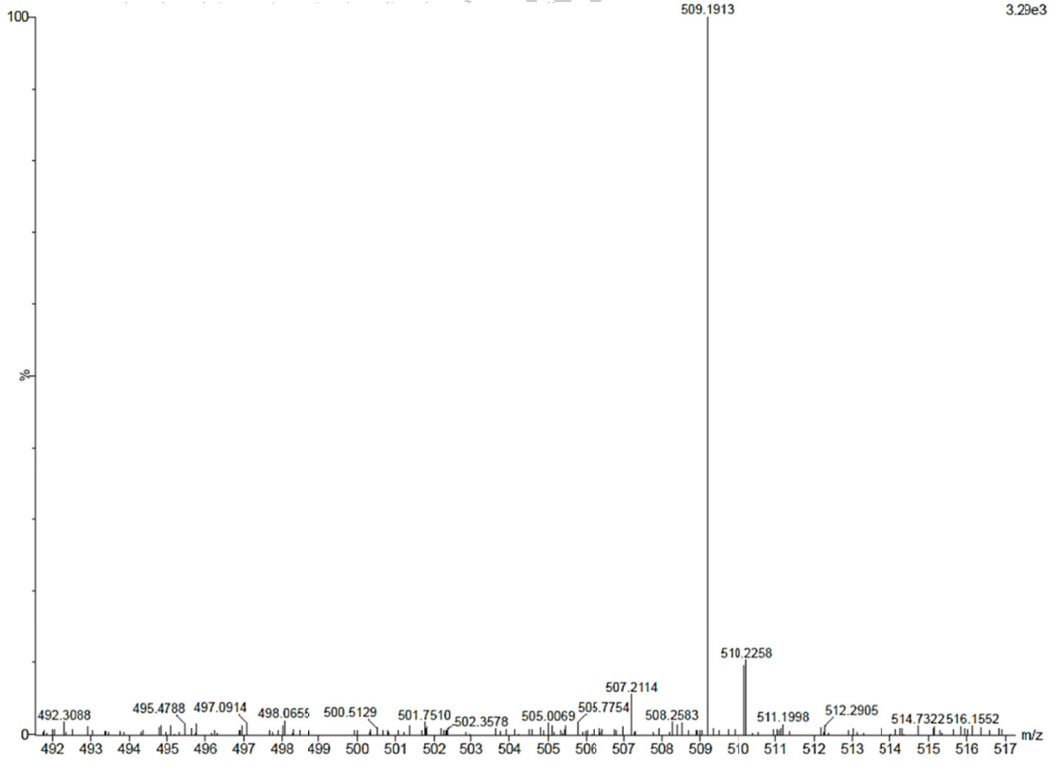

Figure S14. ESI-MS spectrum of **C3** in the presence of FA. Mass (*m/z*) calculated for $C_{34}H_{24}N_2O_3$ $[M + H]^+$ = 509.1820; observed = 509.1913.

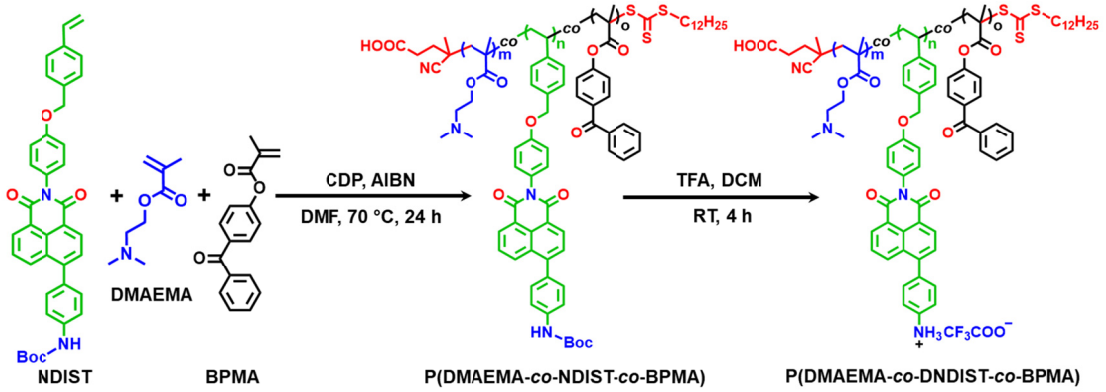

Scheme S2. Synthetic scheme for the preparation of BPMA-containing fluorescent polymeric probe.

Table S1. Characterization of different copolymers synthesized at 70 °C in DMF.

Polymer	% of NDIST in feed	Conv.[b] (%)	% of NDIST in copolymer[c]	$M_{n,theo}$[c] (g/mol)	$M_{n,NMR}$[d] (g/mol)	$M_{n,SEC}$[e] (g/mol)	$Đ$[e]
BCP5[a]	5	70	4	12250	14900	12200	1.21
BCP10[a]	10	64	7	13100	17000	13600	1.18

[a][Monomers]/[CDP]/[AIBN] = 100:1:0.2. For all the reactions, time = 24 h. [b]Conversion (Conv.) was determined by gravimetric analysis. [c]$M_{n,theo}$ = ([Monomers]/[CDP] × (molecular weight (*MW*) of monomer) × Conv. + *MW* of CDP), where *MW* of monomer = average molecular weight considering feed mol% of monomers. [d]Calculated from ^{1}H NMR analysis. [e]Obtained by SEC analysis.